

Tunneling via individual electronic states in ferromagnetic nanoparticles

S. Guéron, Mandar M. Deshmukh, E. B. Myers, and D. C. Ralph
Laboratory of Atomic and Solid State Physics, Cornell University, Ithaca, NY 14853
(October 7, 2018)

We measure electron tunneling via discrete energy levels in ferromagnetic cobalt particles less than 4 nm in diameter, using non-magnetic electrodes. Due to magnetic anisotropy, the energy of each tunneling resonance shifts as an applied magnetic field rotates the particle's magnetic moment. We see both spin-increasing and decreasing tunneling transitions, but we do not observe the spin degeneracy at small magnetic fields seen previously in non-magnetic materials. The tunneling spectrum is denser than predicted for independent electrons, possibly due to spin-wave excitations.

PACS numbers: 73.20.Dx, 75.60.-d, 73.23.Hk

The forces that determine the electronic properties of semiconductor quantum dots or metal nanoparticles can be investigated in a particularly direct, fundamental way through tunneling measurements of the discrete “electrons-in-a-box” spectrum of energy levels. This technique has been used to study the quantum-Hall-effect regime [1], superconducting pairing in aluminum particles [2,3], and effects of more generic electron-electron interactions [4–7]. In this Letter we turn to a ferromagnetic material (cobalt), with the aim of probing the ways in which strong exchange interactions and magnetic anisotropy affect the discrete electron spectrum, as well as investigating spin-polarized tunneling via single quantum states. Our work may be viewed as an extension to smaller size and/or lower temperature of previous experiments employing micron-size ferromagnetic islands [8] and nm-scale cobalt particles [9]. We find a number of phenomena different from past studies of non-magnetic nanoparticles. We observe that the energy levels are coupled to the direction of the particle's total magnetic moment, such that the levels shift as the moment is reoriented. As might be expected, there is no degeneracy in Co between spin-up and spin-down tunneling levels near zero magnetic field, H . The energy spacing of the resonances is smaller than expected in an independent-electron model, suggesting the importance of low-energy many-body spin excitations.

Our samples consist of Co particles connected to Al leads via tunnel barriers. The fabrication is similar to previous work on Al particles [10], and a schematic sample cross-section is shown in Fig. 1(a). The top Al electrode is deposited first so as to fill a bowl etched through a Si_3N_4 membrane (hole radius < 5 nm), and then a tunnel barrier is formed by oxidizing the Al. The Co nanoparticles are obtained by evaporation at room temperature of a Co layer 0.5 nm thick. Surface tension causes the Co to form electrically separate particles. Scanning transmission electron microscope (STEM) images of test samples in which 0.5 nm of Co is deposited on oxidized aluminum indicate Co particles with diameters 1–4 nm, with center-to-center spacing 2–5 nm (Fig. 1(b)).

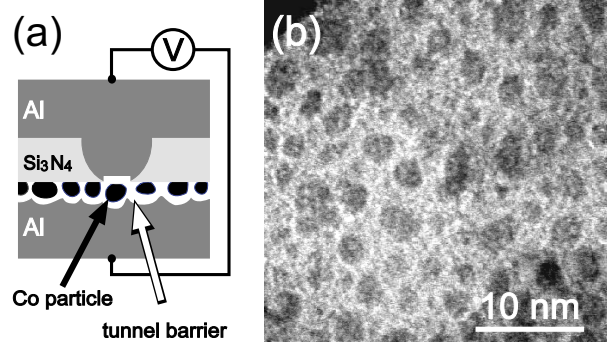


FIG. 1. (a) Cross-sectional device schematic. (b) Annular dark-field plan-view STEM image of Co particles.

The crystal structure was not determined. The second tunnel barrier is formed on the Co particles either by depositing a 0.8 nm-thick layer of Al at 77 K, which we oxidize in 50 mTorr of O_2 for 3 min at room temperature (sample 1), or by directly depositing 1.1 to 1.5 nm of Al_2O_3 (samples 2,3). Finally a thick layer of Al is deposited to make the second electrode. We select devices for which the current-voltage curve at 4.2 K shows Coulomb staircase structure (not shown), indicating tunneling via nanoparticles [11].

Figure 2 shows the tunneling spectra at the onset of conduction for the first Coulomb threshold, for three samples. The spectra consist of well-resolved peaks due to tunneling via discrete electronic levels within each particle, qualitatively similar to previous measurements in Al and Au [10,7]. The values on the energy axis are determined by dividing the voltage by $(C_1+C_2)/C_2$, to correct for capacitive division of the bias, where C_1 and C_2 are the capacitances of the particle to the two electrodes [10]. We can determine this ratio to within 20% by fitting the temperature-dependent broadening of peaks [12], or in one sample having no voltage-dependent charge shifts (sample 2), we can achieve 1% accuracy by comparing the voltages required for tunneling via the same electronic states at positive and negative bias [10]. The peak spacing for all three samples is much less than the Coulomb

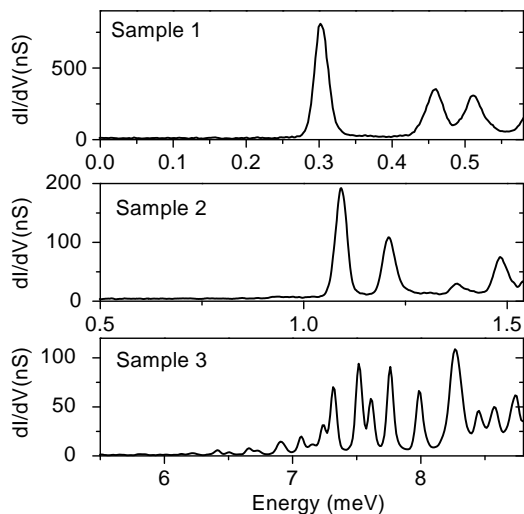


FIG. 2. Tunneling spectra of 3 different samples at $T=20$ mK and $\mu_0 H = 1$ T. H is parallel to the Si_3N_4 membrane. The energy is obtained by dividing V by $(C_1+C_2)/C_2 = 1.2, 2.17$ and 2.5 , respectively, for the three samples.

charging energy (> 30 meV, based on particle size), so that all peaks in each spectrum correspond to tunneling via states with the same number of electrons, either one more or one less than the initial state.

Unlike non-magnetic particles where the energy levels have a simple linear dependence on H due to the spin Zeeman energy [10], the levels in Co have a strong, non-linear dependence on H for small H . Figure 3(a) shows the energy of the first three tunneling resonances of sample 1, as $\mu_0 H$ was swept about a hysteresis loop from -0.45 T to 0.45 T and back again. Starting at -0.45 T (thick lines), the tunneling energies shift in a continuous manner as the field is ramped to zero and the magnetic moment vector \vec{m} of the particle relaxes toward its easy direction. As the field is ramped further, we observe a sudden jump in all three transition energies, at $\mu_0 H_{\text{sw}} = 0.23$ T. We interpret this jump as due to the reversal of \vec{m} in the single-domain Co nanoparticle [13]. The energy shifts with H are hysteretic with respect to the direction of the field sweep, with the expected symmetry around $H = 0$, and the scans are repeatable over days. The value of H_{sw} is comparable to SQUID measurements of 25 ± 5 nm diameter Co particles [14], and corresponds to an anisotropy energy density of order $K=10^5$ J/m³.

These curves indicate a significant coupling between the level energies and the orientation of the magnetic moment of the nanoparticle. Let us consider the simplest model for this anisotropy, so as to see what features of the data may be explained simply, and what features may require deeper understanding. We call the operator for the total electronic spin with N electrons $\hbar\vec{S}(N)$, and we assume that the anisotropy and Zeeman energies are sufficiently weak relative to the exchange splitting between different spin multiplets that the magnitude S in the ground state remains

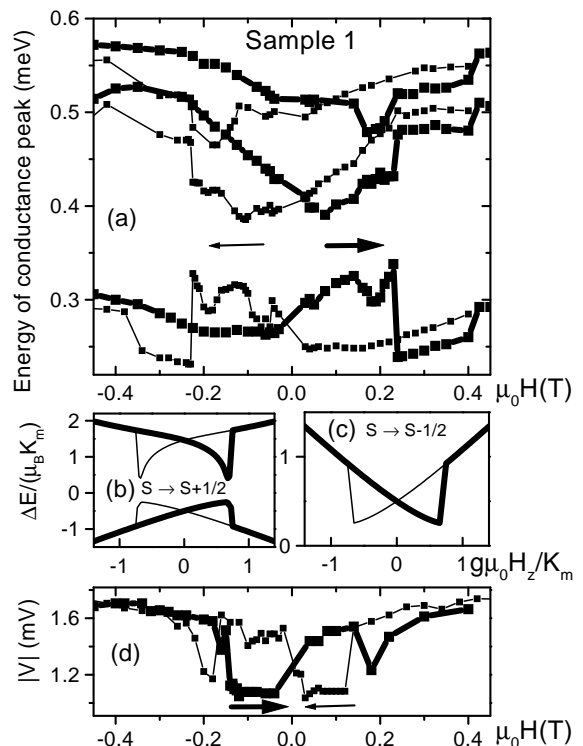


FIG. 3. (a) Hysteresis curves showing the dependence of tunneling energies on H for sample 1, at $T=20$ mK. (b,c) Lowest-energy transitions calculated using the Hamiltonian discussed in text, for $S=50$ and H oriented 45° from the easy axis, for the case where S increases during tunneling (b) and decreases (c). The qualitative features are independent of the value of S . (d) Voltage threshold for tunneling in one sample which exhibits anti-hysteretic behavior.

constant as H is varied, so that we can perform our calculation in the space of this one spin multiplet. (In a classical language this corresponds to assuming that the ground state magnetic moment $\vec{m}(N)$ simply rotates as a function of H .) Including the Zeeman energy and the simplest model of easy-axis anisotropy in the \hat{z} direction [15], the H -dependent terms in the Hamiltonian within the ground-state multiplet for N electrons can be written

$$\mathcal{H} = -g_{\text{eff}}\mu_B\mu_0\vec{H} \cdot \vec{S} - K_m\mu_B S_z^2 / \sqrt{S(S+1)} \quad (1)$$

where K_m is an anisotropy energy per unit $|\vec{m}|$. ($K_m \equiv K(\text{volume})/|\vec{m}|$.) We have omitted from Eq. 1 the charging energy, which we assume to be independent of H . For given total spin values in the N and $N \pm 1$ -electron states, we diagonalize the Hamiltonian numerically to find the energy levels, and then calculate the allowed tunneling transition energies as $E(N \pm 1, H) - E(N, H)$. We allow the moment vector of the nanoparticle to undergo reversal at the classical switching field, which depends on the angle between \vec{H} and the easy axis. Representative results for the lowest-energy tunneling transitions are shown in Fig. 3(b) for the case that S increases during tunneling, and in Fig. 3(c) for S decreasing. The

model successfully reproduces the hysteretic energy maxima near zero field observed in the lowest energy transition (with S increasing), as well as the existence and the sign of the abrupt switching to lower energy at H_{sw} . If we define S_H as the component of the total electron spin in the direction of \vec{H} , in general we find that tunneling transitions in which $\langle S_H \rangle$ increases give maxima near $H=0$ and transitions decreasing $\langle S_H \rangle$ give minima. We can identify both types of behavior in Fig. 3(a). We have also solved the classical analogue of the model, which gives similar results for the ground-state to ground-state transitions.

The measured tunneling energies often have small-scale non-monotonic variations as a function of H that are not present in our minimal model. A likely cause is magnetic interactions between nearby Co particles. The most dramatic example we have observed is shown in Fig. 3(d), where we plot the H -dependence of the threshold voltage for tunneling via a Co nanoparticle too large for discrete resonances to be observed. We see anti-hysteresis – magnetization reversal occurs before H changes sign. This can be explained by the influence of a dipolar magnetic field oriented opposite to the applied H , produced by a second magnetic nanoparticle adjacent to the one through which electron tunneling occurs. The reversed field from the second particle can shift the hysteresis curve of the first so that its value of H_{sw} can be negative, while the non-monotonic shifts at large positive H (0.2 T) are understood as the magnetization reversal of the second particle. A dipole field 5 nm from the center of a 3-nm-diameter Co particle is of order 0.1 T, so that Zeeman interactions alone are not strong enough to explain the level shifts that we observe.

A second departure of the data from the minimal model is that in some cases the model fails to describe the combined low and high H variations of the transition energies (Fig. 4). At large H , the simple model predicts a linear extension of the low field curves, with the tunneling energies Zeeman-shifting as $\pm g_{\text{eff}} \mu_B \mu_0 H / 2$. Figure 4(a) shows that at large H the ground state transition of sample 1 moves to higher energies with increasing H , indicative of a tunneling transition in which $\langle S_H \rangle$ decreases, whereas the low-field behavior indicates a $\langle S_H \rangle$ -increasing transition. Similarly, the ground state transition of sample 2 (Fig 4(b)) is $\langle S_H \rangle$ -decreasing at low field (dip to lower energy) but $\langle S_H \rangle$ -increasing at high field (energy shift to lower energies). We see two possible explanations. Either (i) the true form of the anisotropy is more complicated than assumed in Eq. (1), such that K_m fluctuates to have different values for different spin multiplets, or (ii) contrary to our model's other initial assumption, the total spins of the ground-states for N and $N \pm 1$ electrons are *not* independent of H , so that \vec{S} (classically, \vec{m}) does not simply rotate as H is ramped. The second possibility would mean that the spin character of the many-body

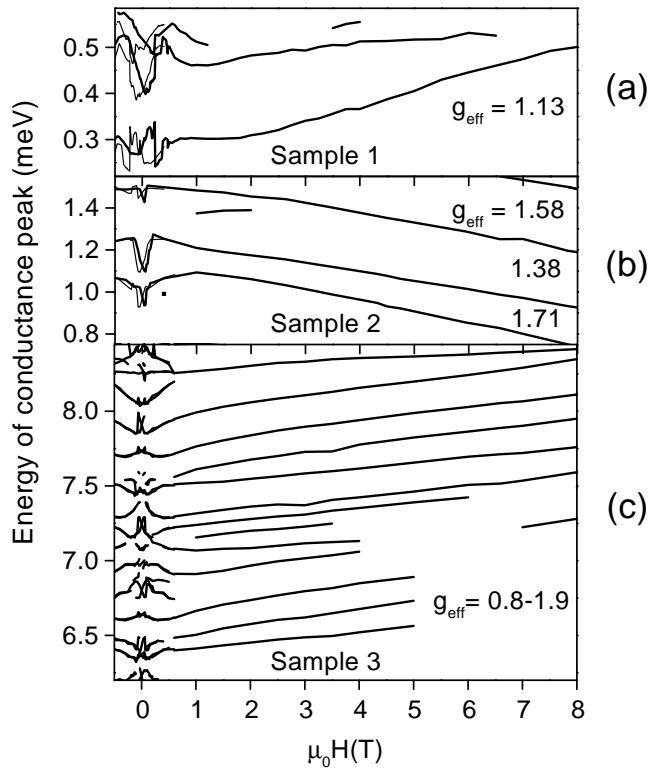


FIG. 4. Tunneling energies over a larger range of H .

electron ground states could evolve with H , so it is possible that the threshold events for tunneling may consist of $\langle S_H \rangle$ -increasing transitions for some values of H , and $\langle S_H \rangle$ -decreasing transitions elsewhere.

For $\mu_0 H > 2$ T, all measurable transition energies within a given sample have the same sign of shift as a function of H . This is different from results in Al and Au nanoparticles, for which Zeeman spin splitting of each orbital state gives rise to both upward and downward-trending states vs. H , with comparable conductance amplitudes, and with a degeneracy at $H = 0$. The absence of spin degeneracy is not surprising in Co, since the exchange field breaks the symmetry between spin-up and down. However, since Co is not fully spin-polarized ($P \approx 30\%$, [16]), the absence of observed peaks shifting in both directions is an indication that electrons do not couple equally well to all allowed many-body energy levels. One factor may be that Clebsch-Gordan coefficients will be very different for $\langle S_H \rangle$ -increasing and $\langle S_H \rangle$ -decreasing transitions in a system with a large ground-state value of the total electron spin, so that some tunneling matrix elements may be immeasurably weak. Note that there is a sign difference between the large- H slopes for sample 2 and those of samples 1 and 3. This might reflect a difference between electron-addition and electron-removal tunneling processes, a possibility which could be tested by fabrication of gated devices.

We wish to distinguish the linear dependence on H that we measure for the tunneling resonances at large H

from the linear shift in the chemical potential of micron-scale Co islands described by Ono *et al.* [8]. The data of [8] can be understood in terms of level crossings in a magnetic island with a continuum of energy states. As H is ramped, spin-up levels cross with spin-down on account of the Zeeman energy, and because the densities of the spin levels are different, more states move one way than the other and the chemical potential must shift. This model is not applicable in explaining the shifts of the *individual* levels that we observe, because in our case any level crossings should be individually resolvable. Quantitatively, the shifts examined by Ono *et al.* in Co correspond to an effective g-factor of 0.7 [8], smaller than the values we measure. (See Fig. 4.)

Finally, we turn to the measured density of tunneling resonances shown in Fig. 2. For the range of particle sizes imaged by STEM, 1-4 nm in diameter, the average level spacing predicted for simple non-interacting electrons should be between 0.75 and 40 meV, given the calculated density of states (including both sp and d bands) in Co of $0.88 \text{ eV}^{-1}\text{atom}^{-1}$ [17]. In our measured spectra, the energy spacing between tunneling peaks is less than 0.2 meV. Enhanced densities of tunneling resonances have previously been seen in Al nanoparticles for values of voltage much greater than the single-electron level spacing, and they were explained as an effect of non-equilibrium electron-hole excitations within the particle [6]. The data in Fig. 2 for samples 1 and 2 are different from the Al results, however, in that an increased density of levels is observed for energies even below the expected single-electron spacing, where electron-hole excitations should not be produced during tunneling. As explanation, we note that electron excitations within a Co nanoparticle may include low-energy spin waves in addition to the independent-electron-type excitations seen in Al. Inelastic emission of spin waves during tunneling may directly contribute new tunneling peaks, and/or non-equilibrium spin excitations generated during tunneling may produce extra tunneling peaks by shifting single-electron states [6]. As a check, we can estimate the minimum energy needed to excite spin-wave modes. For a spatially uniform mode ($k=0$), the excitation energy can be calculated using the anisotropy term in Eq. (1), to be $\approx 2K_m\mu_B$. If we use the size of the jump in the tunneling energy at H_{sw} , $\Delta E \approx 0.05 \text{ meV}$ (Fig. 3) to estimate K_m (using $\Delta E \approx \mu_B K_m$, see Fig. 3(b,c)), we arrive at a value of 0.1 meV for the spin-wave energy, which would explain the enhanced density of tunneling states. The contribution of exchange energy to the lowest-energy *non-uniform* spin-wave modes can be estimated by quantizing the spin-wave dispersion curve of Co within the size of a nanoparticle. This gives an energy $(300 \text{ meV})(a/d)^2$ where a is a lattice spacing and d is the particle diameter [18], or $\approx 1 \text{ meV}$ for a 4-nm particle.

In conclusion, we have measured discrete tunneling res-

onances in nm-scale ferromagnetic Co particles. Magnetic anisotropy causes each resonance energy to shift reproducibly by on the order of 0.1 meV as H is swept about the hysteresis loop. This effect may provide a means to probe the dynamics of magnetization reversal in nm-scale particles, complementary to magnetic force microscopy [19], Hall magnetometry [20], and SQUID techniques [14]. Qualitative features of these shifts can be described by a simple model. However, a full explanation of the measurements will require a more detailed understanding of the electronic states inside a ferromagnet, including at least the contributions of low-energy collective spin-wave excitations to the electron states, and effects of Clebsch-Gordan coefficients in tunneling.

We thank C. T. Black, F. Braun, R. A. Buhrman, M. H. Devoret, H. Hurdequint, J. A. Katine, A. Pasupathy, D. Salinas, J. Silcox, Y. Suzuki, M. Thomas, S. Upadhyay, and J. von Delft. Support: ONR N00014-97-1-0745, NSF DMR-9705059, Packard Foundation, and the Cornell Nanofabrication Facility.

-
- [1] For a review, see R. C. Ashoori, *Nature* **379**, 413 (1996).
 - [2] C. T. Black, D. C. Ralph, and M. Tinkham, *Phys. Rev. Lett.* **76**, 688 (1996); **78**, 4087 (1997).
 - [3] F. Braun and J. von Delft, *Phys. Rev. Lett.* **81**, 4712 (1998), and references therein.
 - [4] S. Tarucha *et al.*, *Phys. Rev. Lett.* **77**, 3613 (1996).
 - [5] D. R. Stewart *et al.*, *Science* **278**, 5344 (1998).
 - [6] O. Agam *et al.*, *Phys. Rev. Lett.* **78**, 1956 (1997).
 - [7] D. Davidović and M. Tinkham, *Phys. Rev. Lett.* **83**, 1644 (1999).
 - [8] K. Ono, H. Shimada, and Y. Ootuka, *J. Phys. Soc. Jap.* **66**, 1261 (1997); **67**, 2852 (1998).
 - [9] L. F. Schelp *et al.*, *Phys. Rev. B* **56**, R5747 (1997); R. Desmicht *et al.*, *Appl. Phys. Lett.* **72**, 386 (1998).
 - [10] D. C. Ralph, C. T. Black, and M. Tinkham, *Phys. Rev. Lett.* **74**, 3241 (1995).
 - [11] At large voltages, more than one nanoparticle contributes to the current in each sample, so that the Coulomb staircase curves cannot be used to estimate capacitances. At the low voltages shown in Fig. 2, only one particle contributes because of Coulomb blockade in the others.
 - [12] C. T. Black, Ph.D. thesis, Harvard University, 1996.
 - [13] Sudden shifts in the chemical potential of micron scale magnetic particles for H comparable to the coercive field have been reported by Ono *et al.* [8].
 - [14] W. Wernsdorfer *et al.*, *Phys. Rev. Lett.* **78**, 1791 (1997).
 - [15] see, *e.g.*, B. D. Cullity, *Introduction to Magnetic Materials*, (Addison-Wesley, Reading, MA, 1972) Ch. 7.
 - [16] R. Meservey and P. M. Tedrow, *Phys. Rep.* **238**, 173 (1994).
 - [17] D. A. Papaconstantopoulos, *Handbook of the Band Structure of Elemental Solids* (Plenum, NY, 1986).
 - [18] N. W. Ashcroft and N. D. Mermin, *Solid State Physics* (Holt, Philadelphia, 1976) p. 709.
 - [19] M. Lederman *et al.*, *Phys. Rev. Lett.* **73**, 1986 (1994).
 - [20] J. G. S. Lok *et al.*, *Phys. Rev. B* **58**, 12201 (1998).